JOURNAL OF APPLIED ELECTROCHEMISTRY **27** (1997) 1333–1342

An integral equation approach for the analysis of current density distribution controlled by diffusion, convection and migration

Z. H. QIU*, L. C. WROBEL‡, H. POWER*,§

*Wessex Institute of Technology, Ashurst Lodge, Ashurst, Southampton SO40 7AA, Great Britain
‡Brunel University, Department of Mechanical Engineering, Uxbridge, Middlesex UB8 3PH, Great Britain
§On leave from: Instituto de Mecánica de Fluídos, Universidad Central de Venezuela, Caracas, Venezuela

Received 10 May 1996; revised 8 April 1997

The present work describes novel numerical formulations based on integral equations for calculating steady-state distributions of concentration, potential and current density in two-dimensional multiple-ion electrochemical systems involving diffusion, convection and migration effects. For simplicity, the electrolyte solutions are considered to be dilute and at a constant temperature. Numerical procedures using the boundary element method (BEM) have been developed specifically for the problem, and are briefly described in the text. The accuracy and efficiency of these procedures are assessed with several tests, involving binary and three-ion systems, linear and non-linear boundary conditions, and problems that are either diffusion- or convection-dominated, or both.

Keywords: *current density distribution*, *diffusion*, *convection*, *migration*, *boundary element method*

List of symbols

c_k	concentration of species k ($\mathrm{mol\,m^{-3}}$)
D_k	diffusion coefficient of species k ($\mathrm{m^2\,s^{-1}}$)
F	Faraday constant ($\mathrm{A\,s\,mol^{-1}}$)
i^*	exchange current density ($\mathrm{A\,m^{-2}}$)
J	current density ($\mathrm{A\,m^{-2}}$)
J_{lim}	limiting current density ($\mathrm{A\,m^{-2}}$)
$\overline{N}_k$	flux density of species k ($\mathrm{mol\,m^{-2}\,s^{-1}}$)
Pe	Péclet number
t	time (s)
q	normal derivative of concentration ($\mathrm{mol\,m^{-4}}$)
u_k	mechanical mobility of species k ($\mathrm{m^2\,mol\,J^{-1}s^{-1}}$)
U	electrical potential (V)
∇U	electrical field ($\mathrm{V\,m^{-1}}$)
v	velocity of the solvent ($\mathrm{m\,s^{-1}}$)
V	voltage (V)
R	gas constant ($\mathrm{J\,mol^{-1}\,K^{-1}}$)
T	absolute temperature (K)
x, y	Cartesian coordinates (m)
z_k	charge number of species k

Greek symbols

α	transfer coefficient
ξ	source point
ρ	electrolyte density ($\mathrm{kg\,m^{-3}}$)
μ	electrolyte viscosity ($\mathrm{kg\,m^{-1}s^{-1}}$)
χ	field point

Subscripts

a	anode
b	boundary point
c	cathode, concentration
fd	first derivative
i	internal point
k	species k
sd	second derivative
v	electrical potential

1. Introduction

Computational electrochemistry is a rapidly developing field centred on three basic theories describing the mass and ion transport processes in electrochemical systems: potential theory, Nernst layer theory and Nernst–Planck theory [1]. The potential theory, being the simplest from the mathematical point of view, is widely applied in theoretical investigations of ionic transport and current distribution. Much work has been done in recent years in the analysis of different electrochemical processes with alternative analytical and numerical methods like the more traditional finite difference method (FDM), the finite element method (FEM) and, more recently, the boundary element method (BEM) [2–7].

To assure a uniform conductivity, the presence of inert supporting electrolyte is necessary. But there is a notable absence of inert ions in redox membranes used as modifiers of electron conductivity electrodes, in solid and liquid ion exchange membranes, and in mixed conductor sandwich cells between metals or between bathing electrolytes, or one of each. Likewise, thin layer electrolytes between metals need not contain supporting electrolyte. In all these cases, there is an enhancement of the steady-state current

0021-891X

and potential theory is no longer valid [8]. A more complicated model, based on Nernst layer theory, is then actively used by many researchers [9–13].

For modelling narrow gap cells, determining the current distribution on small features within the diffusion layer or, in general, for cells with concentration gradients extending over a significant portion of the cell region, the Nernst layer approximation is no longer valid. In this area, when convective effects are not negligible, which often occurs in practice, the diffusion, convection and migration effects must be simultaneously considered. So, the Nernst–Planck transport equation has to be taken into account. Although studies of current distribution have reached a very high level with the aid of powerful computers, solutions of the Nernst–Planck model hardly appeared. So far, only Georgiadou and Alkire [14] published results based on this model, using the finite difference method.

The main objective of the present work is to apply BEM formulations to solve the Nernst–Planck model for predicting concentration, current and potential distributions in electrochemical systems. The main theoretical aspects and numerical algorithms of the BEM model have already been presented in detail elsewhere [15], and will only be briefly reviewed here; this paper concentrates on more practical applications to parallel electrochemical cells.

This research forms part of a joint European project on the development and evaluation of methods for prediction of current density distribution in electrochemical cells, under the sponsorship of the Brite–Euram programme. The project involves the development of two different numerical formulations, one being the BEM and the other the Multi-Dimensional Upwind Method (MDUM), the theoretical basis of which has been reported elsewhere [13]. Comparison of results obtained with these two distinct approaches will be presented here.

2. Governing equations

For a dilute solution in a unionized solvent at constant pressure and temperature, the flux density of each ionic species k is given by [1]

$$\overline{N}_k = -u_k z_k F c_k \nabla U - D_k \nabla c_k + c_k \mathbf{v} \tag{1}$$

The symbols are as stated at the outset of this paper. The three terms on the right-hand side of Equation 1 describe the effects of migration, diffusion and convection, respectively.

The total charge per mole ion is its charge number multiplied by the Faraday constant, $z_k F$, and the current density is hence the flux of the ion multiplied by $z_k F$. For all the species, we have

$$J = F \sum_k z_k \overline{N}_k \tag{2}$$

The material balance for a minor component in an electrolyte can be expressed by

$$\frac{\partial c_k}{\partial t} = -\nabla \cdot \overline{N}_k + R_k \tag{3}$$

with $\partial c_k/\partial t$ being the accumulation of species k, $\nabla \cdot \overline{N}_k$ the difference between the input and the output and R_k the production rate of ion k due to homogeneous chemical reactions in the bulk of the solution. In electrochemical systems, reactions are frequently restricted to electrode surfaces, in which case R_k can be considered as zero.

Equations 1 to 3 (with $R_k = 0$) are equivalent to the following set of equations:

$$\frac{\partial c_k}{\partial t} + \mathbf{v} \cdot \nabla c_k = F z_k \nabla \cdot (u_k c_k \nabla U) + \nabla \cdot (D_k \nabla c_k) \tag{4}$$

$$\nabla \cdot \left\{ -F^2 \sum_k z_k^2 u_k c_k \nabla U - F \sum_k z_k D_k \nabla c_k \right\} = 0 \tag{5}$$

where Equation 5 was obtained by considering conservation of charge and the condition of electroneutrality

$$\sum_k z_k c_k = 0 \tag{6}$$

The above set of equations describes the transport of mass and charge in dilute electrochemical solutions. Even in the simple case of an infinite dilute solution, a complex set of coupled partial differential equations has to be dealt with.

In what follows, only the case of dilute solutions is considered, hence the concentration of species does not affect the velocity field. Thus, the fluid mechanics can be studied separately from the electrochemical analysis, which means that the convective velocity is known in the present case and Equations 4 to 6 can be solved for the unknown variables U and c_k.

3. Numerical formulation

3.1. *Mathematical model*

For two-dimensional steady-state problems, assuming that reactions are restricted to the electrodes and that the coefficients u_k, z_k and D_k are all constant, Equations 4 and 5 can be expressed in the form:

$$D_k \nabla^2 c_k - \left(v_x - F z_k u_k \frac{\partial U}{\partial x} \right) \frac{\partial c_k}{\partial x} - \left(v_y - F z_k u_k \frac{\partial U}{\partial y} \right) \frac{\partial c_k}{\partial y} = -\left(F z_k u_k \nabla^2 U \right) c_k \tag{7}$$

$$\left(\sum_k z_k^2 u_k c_k \right) \nabla^2 U + \left(\sum_k z_k^2 u_k \frac{\partial c_k}{\partial x} \right) \frac{\partial U}{\partial x} + \left(\sum_k z_k^2 u_k \frac{\partial c_k}{\partial y} \right) \frac{\partial U}{\partial y} = -\frac{1}{F} \sum_k z_k D_k \nabla^2 c_k \tag{8}$$

For the purpose of deriving a numerical algorithm employing the boundary element method, the velocity field is initially divided into an average and a perturbation as follows:

$$v_x(x,y) = \overline{v}_x + P_x(x,y) \qquad v_y(x,y) = \overline{v}_y + P_y(x,y)$$

where $\overline{v}_x$ and $\overline{v}_y$ represent the mean (constant) velocity, and P_x, P_y represent the deviation from the

mean at each point. Equation 7 can then be rewritten in the form:

$$D_k\nabla^2 c_k - \overline{v}_x\frac{\partial c_k}{\partial x} - \overline{v}_y\frac{\partial c_k}{\partial y} = P_{cx_k}\frac{\partial c_k}{\partial x} + P_{cy_k}\frac{\partial c_k}{\partial y} + C_{xy_k}c_k \tag{9}$$

with

$$P_{cx_k}(x,y) = P_x - K_k\frac{\partial U}{\partial x}$$
$$P_{cy_k}(x,y) = P_y - K_k\frac{\partial U}{\partial y}$$
$$C_{xy_k}(x,y) = -K_k\nabla^2 U$$
$$K_k = Fz_ku_k$$

Similarly, Equation 8 is rewritten in the form:

$$\nabla^2 U - \overline{v}_{ux}\frac{\partial U}{\partial x} - \overline{v}_{uy}\frac{\partial U}{\partial y} = P_{ux}\frac{\partial U}{\partial x} + P_{uy}\frac{\partial U}{\partial y} + U_{xy} \tag{10}$$

where the terms $\sum_k z_k^2u_k\partial c_k/\partial x$ and $\sum_k z_k^2u_k\partial c_k/\partial y$ in Equation 9 can be interpreted as a kind of convective velocity, and hence also divided into an average and a perturbation:

$$v_{ux}(x,y) = \overline{v}_{ux} + P_{ux}(x,y)$$
$$v_{uy}(x,y) = \overline{v}_{uy} + P_{uy}(x,y)$$

with

$$v_{ux}(x,y) = -\left(\sum_k z_k^2u_k\frac{\partial c_k}{\partial x}\right)\Bigg/\left(\sum_k z_k^2u_kc_k\right)$$
$$v_{uy}(x,y) = -\left(\sum_k z_k^2u_k\frac{\partial c_k}{\partial y}\right)\Bigg/\left(\sum_k z_k^2u_kc_k\right)$$
$$U_{xy}(x,y) = -\left(\sum_k z_kD_k\nabla^2 c_k\right)\Bigg/\left(F\sum_k z_k^2u_kc_k\right)$$

It is important to notice that, while the terms $\overline{v}_x$ and $\overline{v}_y$ in Equation 9 correspond to a known velocity field, the terms $\overline{v}_{ux}$ and $\overline{v}_{uy}$ in Equation 10 are dependent on the unknown concentrations c_k.

The iterative scheme of solution of the system starts by fixing an initial variation for the electrical potential U, and solving a set of Equations 9 for $K-1$ concentrations using the BEM. This solution provides values of c_k and $\partial c_k/\partial n$ along the boundary. With these values it is then possible to directly calculate values of c_k at internal points, first derivatives of c_k at boundary and internal points, and second derivatives of c_k at internal points. The values of concentration and derivatives of the last ion are obtained using Equation 6 and its derivatives.

Next, Equation 10 is solved for U using the previously calculated distributions of c_k and their derivatives to evaluate v_{ux}, v_{uy} and U_{xy}. Initially, a boundary element scheme is used to calculate U and $\partial U/\partial n$ along the boundary. Thus, values of $\partial U/\partial x, \partial U/\partial y$ and $\nabla^2 U$ at internal points can be evaluated explicitly. These are then used to give a better estimate of the concentrations c_k by solving Equation 9 again. This procedure is repeated until convergence is achieved for all concentrations c_k and U.

3.2. *BEM formulation for multiple-ion electrochemical systems*

The fundamental solution of the two-dimensional steady-state diffusion-convection equation with constant velocity field

$$D\nabla^2 c - \overline{v}_x\frac{\partial c}{\partial x} - \overline{v}_y\frac{\partial c}{\partial y} = 0$$

is of the form [15]

$$c^*(\xi,\chi) = \frac{1}{2\pi D}\mathrm{e}^{-\frac{\overline{\mathbf{v}}\mathbf{r}}{2D}}K_0\left(\frac{|\overline{\mathbf{v}}|r}{2}\right)$$

where $\overline{\mathbf{v}}$ is the velocity vector, ξ and χ represent source and field points, respectively, r is the modulus of $\mathbf{r}$, the distance vector between ξ and χ, and K_0 is the Bessel function of second kind of zero order.

By employing the above fundamental solution and Green's identities, when source points are inside the domain, Equation 9 can be transformed into the following integral equation

$$\begin{aligned} &c(\xi) - D\int_\Gamma c^*(\xi,\chi)\frac{\partial c(\chi)}{\partial n_\chi}\mathrm{d}\Gamma(\chi) \\ &+ D\int_\Gamma \frac{\partial c^*(\xi,\chi)}{\partial n_\chi}c(\chi)\mathrm{d}\Gamma(\chi) + \int_\Gamma c^*(\xi,\chi)\overline{v}_n(\chi)c(\chi)\mathrm{d}\Gamma(\chi) \\ &= -\int_\Omega c^*(\xi,\chi)\left[P_{cx}(\chi)\frac{\partial c(\chi)}{\partial x_\chi} + P_{cy}(\chi)\frac{\partial c(\chi)}{\partial y_\chi}\right. \\ &\qquad\left. + C_{xy}(\chi)c(\chi)\right]\mathrm{d}\Omega(\chi) \end{aligned} \tag{11}$$

where $\overline{v}_n = \overline{\mathbf{v}}\cdot\mathbf{n}$, $\mathbf{n}$ is the unit outward normal vector. For simplification, we will denote by $b = P_{cx}(\partial c/\partial x) + P_{cy}(\partial c/\partial y) + C_{xy}c$ the term within brackets on the right-hand side of Equation 11.

It is important to notice that only the fundamental solution depends on the position of the source point; all other terms are only related to field points. Based on this, it is possible to take derivatives with respect to coordinates of the source point directly on the above Equation 15.

The first derivative of function c with respect to coordinate x of the source point is thus obtained by differentiating Equation 11:

$$\begin{aligned} &\frac{\partial c(\xi)}{\partial x_\xi} - D\int_\Gamma \frac{\partial c^*(\xi,\chi)}{\partial x_\xi}q(\chi)\mathrm{d}\Gamma \\ &+ D\int_\Gamma \frac{\partial^2 c^*(\xi,\chi)}{\partial n_\chi\partial x_\xi}c(\chi)\mathrm{d}\Gamma + \int_\Gamma \frac{\partial c^*(\xi,\chi)}{\partial x_\xi}\overline{v}_n(\chi)c(\chi)\mathrm{d}\Gamma \\ &= -\int_\Omega \frac{\partial c^*(\xi,\chi)}{\partial x_\xi}b(\chi)\mathrm{d}\Omega \end{aligned} \tag{12}$$

The first derivative of function c with respect to coordinate y of the source point is given, analogously:

$$\frac{\partial c(\xi)}{\partial y_\xi} - D\int_\Gamma \frac{\partial c^*(\xi,\chi)}{\partial y_\xi} q(\chi)\mathrm{d}\Gamma + D\int_\Gamma \frac{\partial^2 c^*(\xi,\chi)}{\partial n_\chi \partial y_\xi} c(\chi)\mathrm{d}\Gamma + \int_\Gamma \frac{\partial c^*(\xi,\chi)}{\partial y_\xi} \bar{v}_n(\chi) c(\chi)\mathrm{d}\Gamma = -\int_\Omega \frac{\partial c^*(\xi,\chi)}{\partial y_\xi} b(\chi)\mathrm{d}\Omega \quad (13)$$

A similar procedure can be undertaken for obtaining integral equations for the second derivatives, although care must be taken when differentiating the domain integral because of the strong singularity of the kernel [15].

To obtain a boundary integral representation analogous to Equation 11, the limit is taken when the source point ξ approaches the boundary Γ in Equation 11 producing the expression:

$$\alpha(\xi)c(\xi) - D\int_\Gamma c^*(\xi,\chi)q(\chi)\mathrm{d}\Gamma(\chi) + D\int_\Gamma \frac{\partial c^*(\xi,\chi)}{\partial n_\chi} c(\chi)\mathrm{d}\Gamma(\chi) + \int_\Gamma c^*(\xi,\chi)\bar{v}_n(\chi)c(\chi)\mathrm{d}\Gamma(\chi) = -\int_\Omega c^*(\xi,\chi)b(\chi)\mathrm{d}\Omega(\chi) \quad (14)$$

where $\alpha(\xi)$ is a function of the internal angle subtended at point ξ. In particular, $\alpha = 1/2$ on a smooth boundary.

Equations for the derivatives of c with respect to the coordinates of the source point, for a source point on the boundary, can also be obtained by using similar limiting processes. Again, care must be taken in evaluating the jumps that appear in these limiting processes because of the strong singularity of the kernels; thus, the corresponding surface integrals have to be evaluated in the sense of Cauchy principal value and Hadamard finite parts [15].

3.3. *Numerical solution*

For the numerical solution by the BEM, the boundary is discretized into elements and the domain into cells [16]. The boundary integral Equation 14 for the concentration is applied at each boundary node using a collocation technique, generating a system of equations of the form

$$H_{\mathrm{cb}}C_{\mathrm{b}} - G_{\mathrm{cb}}Q_c = -E_{\mathrm{cb}}B_{\mathrm{c}} \quad (15)$$

In the above system, H_{cb} and G_{cb} are standard influence matrices, E_{cb} is a matrix resulting from the domain integral, C_{b} is the vector of boundary concentrations (for a specific ion), Q_{c} is a vector containing the normal derivatives $\partial c/\partial n$, and B_{c} is a vector containing values of b_{c} at each internal node.

To eliminate the domain variable b_{c} from the system of Equations 15, we start by writing the following equations for the concentration and its first derivatives at internal points, which results from the application of Equations 11–13

$$C_{\mathrm{i}} + H_{\mathrm{c}}C_{\mathrm{b}} - G_{\mathrm{c}}Q_{\mathrm{c}} = -E_{\mathrm{c}}B_{\mathrm{c}} \quad (16)$$

$$\frac{\partial C_{\mathrm{i}}}{\partial x} + H_{\mathrm{cxfd}}C_{\mathrm{b}} - G_{\mathrm{cxfd}}Q_{\mathrm{c}} = -E_{\mathrm{cxfd}}B_{\mathrm{c}} \quad (17)$$

$$\frac{\partial C_{\mathrm{i}}}{\partial y} + H_{\mathrm{cyfd}}C_{\mathrm{b}} - G_{\mathrm{cyfd}}Q_{\mathrm{c}} = -E_{\mathrm{cyfd}}B_{\mathrm{c}} \quad (18)$$

Thus, multiplying Equation 16 by C_{xy}, Equation 17 by P_{cx}, Equation 18 by P_{cy} and adding the resulting equations gives

$$I\,B_{\mathrm{c}} + H_{\mathrm{ci}}C_{\mathrm{b}} - G_{\mathrm{ci}}Q_{\mathrm{c}} = -E_{\mathrm{ci}}B_{\mathrm{c}} \quad (19)$$

Here, I is the unit matrix and

$$H_{\mathrm{ci}} = C_{xy}H_{\mathrm{c}} + P_{\mathrm{cx}}H_{\mathrm{cxfd}} + P_{\mathrm{cy}}H_{\mathrm{cyfd}}$$
$$G_{\mathrm{ci}} = C_{xy}G_{\mathrm{c}} + P_{\mathrm{cx}}G_{\mathrm{cxfd}} + P_{\mathrm{cy}}G_{\mathrm{cyfd}}$$
$$E_{\mathrm{ci}} = C_{xy}E_{\mathrm{c}} + P_{\mathrm{cx}}E_{\mathrm{cxfd}} + P_{\mathrm{cy}}E_{\mathrm{cyfd}}$$

Eliminating the variable b from Equations 15 and 19, another matrix system is constructed,

$$[H_{\mathrm{cb}} - E_{\mathrm{cb}}(E_{\mathrm{ci}} + I)^{-1}H_{\mathrm{ci}}]C_{\mathrm{b}} = [G_{\mathrm{cb}} - E_{\mathrm{cb}}(E_{\mathrm{ci}} + I)^{-1}G_{\mathrm{ci}}]\,Q_{\mathrm{c}} \quad (20)$$

which only relates boundary values. With it, all the boundary unknowns can be evaluated. This step is completed by solving a system of equations. Once all nodal boundary values are obtained, the system of Equations 19 is also solved to provide the domain terms b_{c}. After this, the values of concentration at internal points, and derivatives at boundary and internal points, can be calculated explicitly by using Equations 16–18 and the following [15]:

$$\frac{\partial^2 C_i}{\partial x^2} + H_{\mathrm{cxsd}}C_{\mathrm{b}} - G_{\mathrm{cxsd}}Q_{\mathrm{c}} = -E_{\mathrm{cxsd}}B_{\mathrm{c}} \quad (21)$$

$$\frac{\partial^2 C_i}{\partial y^2} + H_{\mathrm{cysd}}C_{\mathrm{b}} - G_{\mathrm{cysd}}Q_{\mathrm{c}} = -E_{\mathrm{cysd}}B_{\mathrm{c}} \quad (22)$$

$$\frac{\partial C_{\mathrm{b}}}{\partial x} + H_{\mathrm{bxfd}}C_{\mathrm{b}} - G_{\mathrm{bxfd}}Q_{\mathrm{c}} = -E_{\mathrm{bxfd}}B_{\mathrm{c}} \quad (23)$$

$$\frac{\partial C_{\mathrm{b}}}{\partial y} + H_{\mathrm{byfd}}C_{\mathrm{b}} - G_{\mathrm{byfd}}Q_{\mathrm{c}} = -E_{\mathrm{byfd}}B_{\mathrm{c}} \quad (24)$$

3.3.1. Solution for the electrical potential. The set of matrix equations for calculating the electrical potential U is obtained following the same ideas as for the concentration c. These matrices are of the form [15]:

$$H_{\mathrm{ub}}U_{\mathrm{b}} - G_{\mathrm{ub}}Q_{\mathrm{u}} = -E_{\mathrm{ub}}B_{\mathrm{u}} \quad (25)$$

$$\frac{\partial U_{\mathrm{i}}}{\partial x} + H_{\mathrm{uxfd}}U_{\mathrm{b}} - G_{\mathrm{uxfd}}Q_{\mathrm{u}} = -E_{\mathrm{uxfd}}B_{\mathrm{u}} \quad (26)$$

$$\frac{\partial U_{\mathrm{i}}}{\partial y} + H_{\mathrm{uyfd}}U_{\mathrm{b}} - G_{\mathrm{uyfd}}Q_{\mathrm{u}} = -E_{\mathrm{uyfd}}B_{\mathrm{u}} \quad (27)$$

$$\frac{\partial^2 U_{\mathrm{i}}}{\partial x^2} + H_{\mathrm{uxsd}}U_{\mathrm{b}} - G_{\mathrm{uxsd}}Q_{\mathrm{u}} = -E_{\mathrm{uxsd}}B_{\mathrm{u}} \quad (28)$$

$$\frac{\partial^2 U_{\mathrm{i}}}{\partial y^2} + H_{\mathrm{uysd}}U_{\mathrm{b}} - G_{\mathrm{uysd}}Q_{\mathrm{u}} = -E_{\mathrm{uysd}}B_{\mathrm{u}} \quad (29)$$

$$I\,B_{\mathrm{u}} - U_{xy} + H_{\mathrm{ui}}U_{\mathrm{b}} - G_{\mathrm{ui}}Q_{\mathrm{u}} = -E_{\mathrm{ui}}B_{\mathrm{u}} \quad (30)$$

In the above, vectors U_{b} and Q_{u} comprise the values of the electrical potential and its normal derivative, respectively, at boundary nodes; vectors U_{i} and B_{u} comprise the values of U and the term b, respectively, at internal points. The domain variable b for the electrical potential equation is defined in the form

$$b_{\mathrm{u}} = P_{\mathrm{ux}}\frac{\partial U_{\mathrm{i}}}{\partial x} + P_{\mathrm{uy}}\frac{\partial U_{\mathrm{i}}}{\partial y} + U_{xy}$$

The final set of equations for the unknown values of U and $\partial U/\partial n$ on the boundary is obtained by substituting the vector B_u in Equation 25 by its expression in terms of U_b and Q_u, given by Equation 30. The final result is of the form:

$$[H_{ub} - E_{ub}(E_{ui} + I)^{-1}H_{ui}]\,U_b = [G_{ub} - E_{ub}(E_{ui} + I)^{-1}G_{ui}]\,Q_u - E_{ub}(E_{ui} + I)^{-1}U_{xy} \quad (31)$$

where

$$H_{ui} = P_{ux}H_{uxfd} + P_{uy}H_{uyfd}$$
$$G_{ui} = P_{ux}G_{uxfd} + P_{uy}G_{uyfd}$$
$$E_{ui} = P_{ux}E_{uxfd} + P_{uy}E_{uyfd}$$

After solving system (31) and calculating the values of B_u by solving system (30), it is possible to calculate first and second derivatives at internal points, explicitly, using Equations 26 to 29.

3.3.2. Iteration procedure. The iteration procedure is carried out with the following steps:

(i) With an initial estimate of the electrical potential distribution (which can be a null field) calculate P_{cx}, P_{cy} and C_{xy}.
(ii) Solve Equation 20 for the boundary values of c_b and $q_c = \partial c_b/\partial n$ (subscript b means that the source point is on the boundary).
(iii) Calculate the values of b_c at internal points by solving the system (19).
(iv) Calculate the values of $\partial c_b/\partial x$ and $\partial c_b/\partial y$ using Equations 23 and 24.
(v) Calculate the values of c_i, $\partial c_i/\partial x$, $\partial c_i/\partial y$, $\partial^2 c_i/\partial x^2$ and $\partial^2 c_i/\partial y^2$ (subscript i means that the source point is on the domain), using Equations 16–18, 21 and 22.
(vi) Repeat steps 1 to 5 for the concentration of ions 1 to $K-1$.
(vii) Calculate the concentration of ion K, and its derivatives, by enforcing the electroneutrality condition.
(viii) Using the above values, calculate the values of v_{ux}, v_{uy} and U_{xy} and solve the system of Equations 31 to provide a new distribution of U_b and q_u.
(ix) Calculate the values of b_u at internal points by solving the system (30).
(x) Calculate the values of $\partial U_i/\partial x$, $\partial U_i/\partial y$, $\partial^2 U_i/\partial x^2$ and $\partial^2 U_i/\partial y^2$ using Equations 26–29.
(xi) Update the values of P_{cx}, P_{cy} and C_{xy} for each ion, and go to step 2.

Convergence of the solution is verified for all the concentrations and the electrical potential. Thus, it is possible (and likely) that some of the variables will converge faster than others. In this case, the iteration loop proceeds until convergence of the remaining variables is achieved.

In spite of the large number of matrix equations involved in the iteration process, its efficiency is very reasonable. This is because all the matrices depend only on geometry, the diffusion coefficient (which is constant) and the convection coefficients. For the concentration Equation 9, it is recalled that the terms $\bar{v}_x$ and $\bar{v}_y$ correspond to a known velocity field which is constant throughout the iteration steps. However, for the electrical potential Equation 10, the terms v_{ux} and v_{uy} depend on c. The procedure adopted was to maintain the mean values $\bar{v}_{ux}$ and $\bar{v}_{uy}$ from the first iteration constant throughout the process, and only update the perturbation terms P_{ux} and P_{uy}.

4. Applications

To assess the boundary element formulations presented here, simulations are now performed on parallel plate reactors with fully developed laminar parabolic flows. Electrolytes with two or three ions are considered such that binary solutions and solutions with an excessive amount of supporting electrolyte can be modelled.

4.1. *Example 1*

The first example is a simple theoretical problem involving convection, diffusion and migration effects. The electrolyte consists of three ions and ion 1 is taken as reactive. A simple linear boundary condition coupling the concentrations and electrical potential at cathode and anode is imposed. All constants and variables are given in dimensionless form, as follows:

$$F = u_k = D_k = 1, \quad z_1 = 2, \quad z_2 = 1, \quad z_3 = -2$$

for $k = 1, 2, 3$.

A sketch of the parallel plate reactor is shown in Fig. 1. The parabolic velocity field is given by $v_x = 500y(1-y)$, $v_y = 0$. The following boundary conditions are imposed:

at $x = 0$

$$c_1 = 0.5 \quad c_2 = 1 \quad c_3 = 1 \quad \frac{\partial U}{\partial n} = 0$$

at $x = 11$

$$\frac{\partial c_1}{\partial n} = 0\,; \quad \frac{\partial c_2}{\partial n} = 0\,; \quad \frac{\partial c_3}{\partial n} = 0\,; \quad \frac{\partial U}{\partial n} = 0$$

at $y = 0$ and $5 \le x \le 6$

$$2c_1\frac{\partial U}{\partial n} + \frac{\partial c_1}{\partial n} = -0.5$$
$$c_2\frac{\partial U}{\partial n} + \frac{\partial c_2}{\partial n} = 0$$
$$c_3 = c_1 + 0.5\,c_2$$

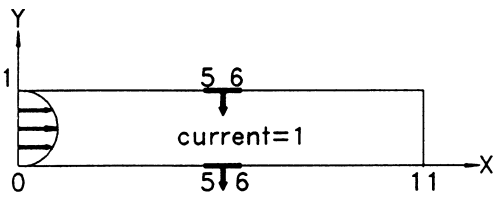

Fig. 1. Sketch of reactor for test 1.

$$\frac{\partial U}{\partial n} = \frac{-0.5}{(2c_1 + 2c_3 + 0.5\,c_2)}$$

at $y = 0$ and $x \leq 5$; $x \geq 6$

$$\frac{\partial c_1}{\partial n} = 0; \quad \frac{\partial c_2}{\partial n} = 0; \quad \frac{\partial c_3}{\partial n} = 0\,; \quad \frac{\partial U}{\partial n} = 0$$

at $y = 0$ and $x = 5.5$

$$U = 0$$

at $y = 1$ and $5 \leq x \leq 6$

$$2c_1 \frac{\partial U}{\partial n} + \frac{\partial c_1}{\partial n} = 0.5$$

$$c_2 \frac{\partial U}{\partial n} + \frac{\partial c_2}{\partial n} = 0$$

$$c_3 = c_1 + 0.5\,c_2$$

$$\frac{\partial U}{\partial n} = \frac{0.5}{(2c_1 + 2c_3 + 0.5\,c_2)}$$

at $y = 1$ and $x \leq 5$; $x \geq 6$

$$\frac{\partial c_1}{\partial n} = 0\,; \quad \frac{\partial c_2}{\partial n} = 0; \quad \frac{\partial c_3}{\partial n} = 0\,; \quad \frac{\partial U}{\partial n} = 0$$

Numerical results obtained for the concentration of ion 1 along the faces $y = 0$ and $y = 1$ are presented in Figs 2 and 3, compared to those obtained using the Multi-Dimensional Upwinding Method (MDUM) [17]. The solutions are in excellent agreement although the numerical methods of solution are totally different. Very similar comparisons were obtained for the concentrations of ions 2 and 3.

This problem, although geometrically simple, presents a mild singularity at the leading edges of the electrodes caused by a discontinuity in the current density distribution, which is generally difficult to treat using numerical methods. A small undershoot in the concentration at the leading edge can be noted in the BEM results of Fig. 2, while a small overshoot is seen in Fig. 3. These are very small errors which can only be appreciated because of the scales adopted in the Figures.

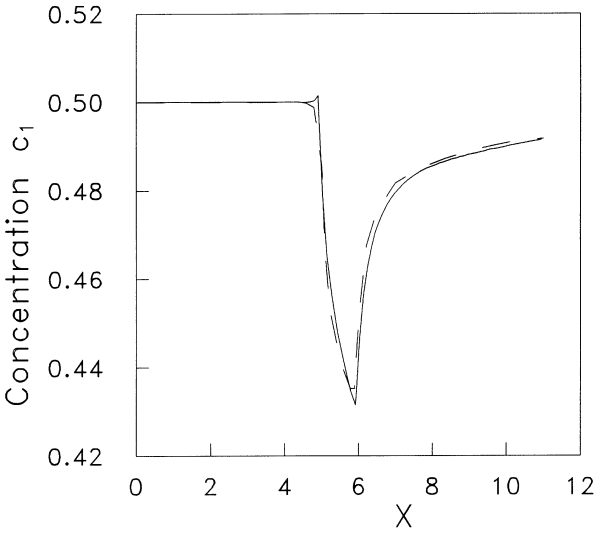

Fig. 3. Variation of concentration c_1 along $y = 0$. BEM results (——); MDUM results (– – –).

To confirm the above statement, we notice that the boundary conditions at the electrolytes are given as Robin conditions for c_1 and c_2, a Dirichlet condition for c_3 and a Neumann condition for the electrical potential U; these should correspond to a constant current density equal to one (the current density is zero at all other faces). By substituting the results obtained for the concentrations, their gradients and the normal derivative of the potential into the general expression (2) for calculating the current density, we found an almost constant current density distribution equal to 0.999 962, with a maximum value of 1.000 12 at the centre of the electrolyte.

The variation of the electrical potential along the top and bottom faces can be seen in Figs 4 and 5, showing again a very good agreement with the MDUM solution.

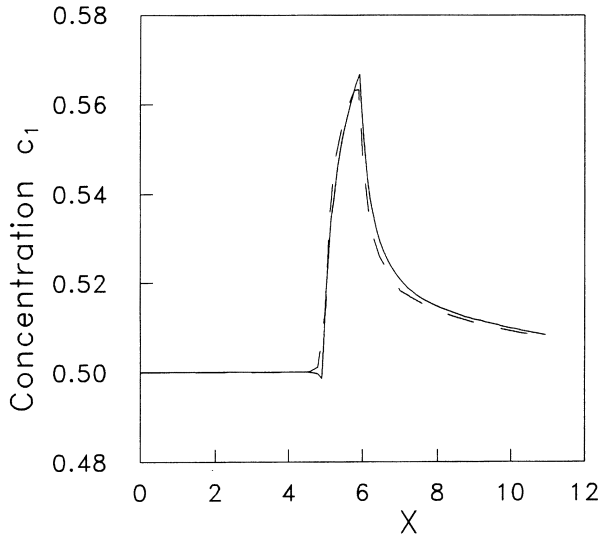

Fig. 2. Variation of concentration c_1 along $y = 1$. BEM results (——); MDUM results (– – –).

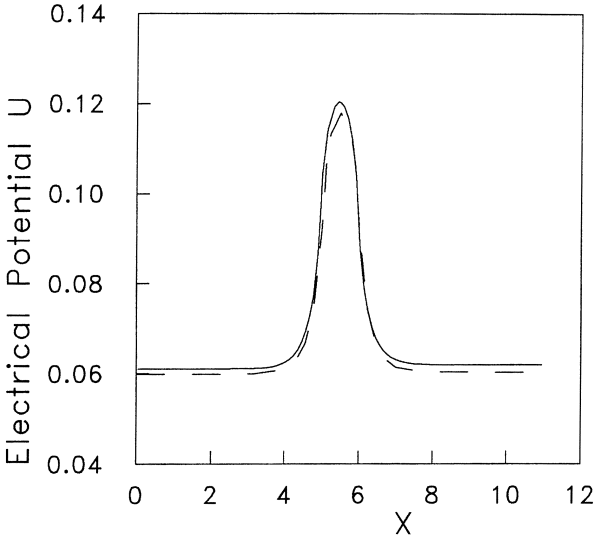

Fig. 4. Variation of potential U along $y = 1$. BEM results (——); MDUM results (– – –).

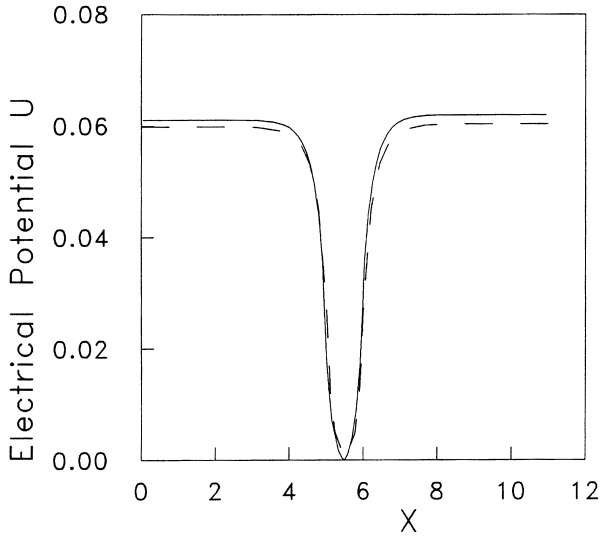

Fig. 5. Variation of potential U along $y = 0$. BEM results (——); MDUM results (– – –).

4.2. *Example 2*

The second test is a problem of diffusion and migration in a binary electrolyte system; no convection is involved in order that analytical solutions can be obtained to compare with the numerical ones. It consists of a parallel plate cell with metal dissolution at the anode ($x = 0$) and metal deposition at the cathode ($x = L$), the geometry of which is shown in Fig. 6.

For both electrode reactions, the following Butler–Volmer polarization equation is applied [1]:

$$J_{na} = i_a^* \frac{c_1}{c_{1b}} \left\{ \exp\left[\frac{\alpha_a F}{RT}(V_a - U)\right] - \exp\left[\frac{-\alpha_c nF}{RT}(V_a - U)\right] \right\}$$

$$J_{nc} = -i_c^* \frac{c_1}{c_{1b}} \left\{ \exp\left[\frac{\alpha_a F}{RT}(V_c - U)\right] - \exp\left[\frac{-\alpha_c nF}{RT}(V_c - U)\right] \right\}$$

in which α is the transfer coefficient.

The following values of constants and physical properties are adopted:

$$i_a^* = i_c^* = 0.01\ \mathrm{A\,cm^{-2}}$$

$$D_1 = D_2 = 10^{-5}\ \mathrm{cm^2 s^{-1}}$$

$$z_1 = 1 \qquad z_2 = -1$$

$$L = 1\ \mathrm{cm} \qquad c_{1b} = 10^{-4}\ \mathrm{mol\,cm^{-3}}$$

$$V_c = 0.0\ V; \qquad \alpha_a = \alpha_c = 0.5$$

$$R = 8.314\ \mathrm{J\,mol^{-1}K^{-1}} \qquad T = 25\ ^\circ\mathrm{C}$$

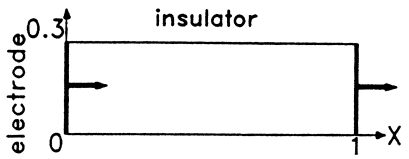

Fig. 6. Sketch of reactor for test 2.

The boundary conditions for this problem are: at $x = 0$

$$c_1 = c_2$$

$$\frac{\partial c_2}{\partial n} = 38.6\, c_2 \frac{\partial U}{\partial n}$$

$$\frac{\partial U}{\partial n} = \frac{2.6846\, c_1}{(c_1 + c_2)} vexp$$

with

$$vexp = \exp[19.47\,(V_c - U)] - \exp[19.47\,(U - V_c)]$$

at $x = 1$

$$c_1 = c_2$$

$$\frac{\partial c_2}{\partial n} = 38.6\, c_2 \frac{\partial U}{\partial n}$$

$$\frac{\partial U}{\partial n} = \frac{2.6846\, c_1}{(c_1 + c_2)} vexp$$

with

$$vexp = \exp[19.47\,(V_a - U)] - \exp[19.47\,(U - V_a)]$$

at $x = 0.5$, $y = 0$ and $y = 0.3$

$$c_1 = c_2 = 10^{-4}\ \mathrm{mol\,cm^{-3}}$$

$$U = D - 0.0596$$

at $y = 0$ and $y = 0.3$:

$$\frac{\partial c_1}{\partial n} = 0; \quad \frac{\partial c_2}{\partial n} = 0; \quad \frac{\partial U}{\partial n} = 0$$

The main difference between this test and the previous one is that the boundary conditions for the potential at the anode and cathode are nonlinear, and the system of equations is thus solved iteratively using a Newton–Raphson technique (see [18] for more details).

Numerical results for different voltages V_a applied at the anode are presented in Figs 7 and 8, and compared to the exact solution given by [17]

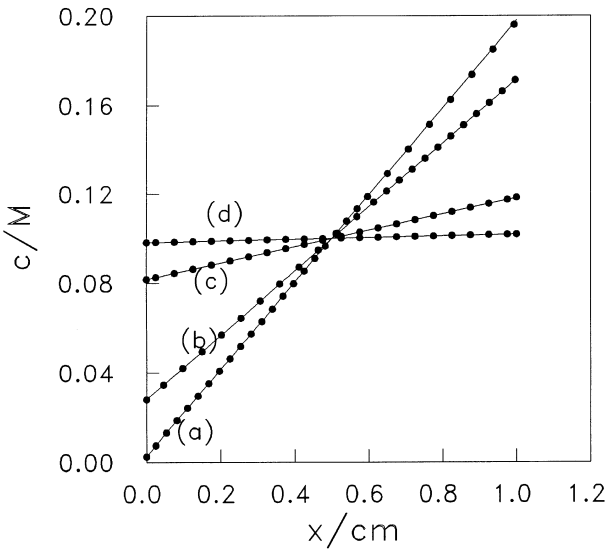

Fig. 7. Comparison between numerical and analytical results for the concentration, for different applied voltages. Analytical results (——); (•) indicates numerical results. (a) $V_a = 0.150$ V; (b) $V_a = 0.050$ V : (c) $V_a = 0.010$ V; (d) $V_a = 0.001$ V.

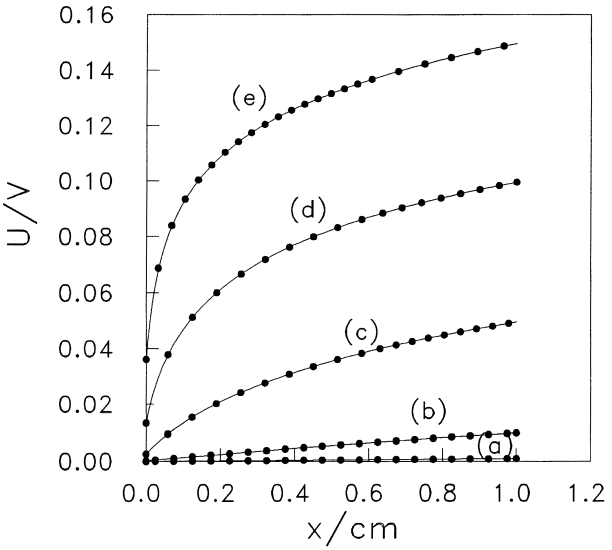

Fig. 8. Comparison between numerical and analytical results for the potential, for different applied voltages. Analytical results (——); (•) indicates numerical results. (a) $V_a = 0.001$ V; (b) $V_a = 0.010$ V: (c) $V_a = 0.050$ V; (d) $V_a = 0.100$ V; (e) $V_a = 0.150$ V.

$$c_1 = c_2 = Ax + B$$
$$U = 0.0257 \ln c_1 + D$$

in which the constants A, B and D are listed in Table 1, as functions of V_a. It can be seen that, although the concentrations vary linearly, the electrical potential has a sharp variation in the neighbourhood of the anode, for high voltages, which is well reproduced by the BEM solution.

4.3. *Example 3*

This is a three ion system consisting of 10^{-5} mol cm^{-3} $CuSO_4$ and 10^{-4} mol cm^{-3} H_2SO_4 in a mass transport situation. Constant velocity is applied in the x-direction with values of 0.003, 0.03, 0.3 and 3 m s^{-1}, respectively. This is not a realistic flow field because of the slip condition at fixed walls; however, this allows a comparison with an analytical solution to be derived next. Because solutions of limiting current density are sought, only the reactive ion c_1 is relevant here. The geometry of the problem is shown in Fig. 9.

The boundary conditions are as follows: $c_1 = 0$ at the cathode; $c_1 = c_b$ at the anode and at the inlet; $\partial c_1/\partial n = 0$ at all other surfaces. The numerical values of the electrolyte properties and constants are as follows: $F = 96\,500$ C mol^{-1}, $n = 2, D = 7.2 \times 10^{-6}$ cm^2 s^{-1}, $c_b = 10^{-5}$ mol cm^{-3}.

Table 1. Parameters for example 2

V_a/V	A	B	D
0.001	3.7161×10^{-6}	9.8142×10^{-5}	2.3912×10^{-1}
0.01	3.6714×10^{-5}	8.1643×10^{-5}	2.4409×10^{-1}
0.05	1.4397×10^{-4}	2.8014×10^{-5}	2.7414×10^{-1}
0.10	1.8615×10^{-4}	6.9237×10^{-6}	3.2108×10^{-1}
0.15	1.9502×10^{-4}	2.4879×10^{-6}	3.7048×10^{-1}

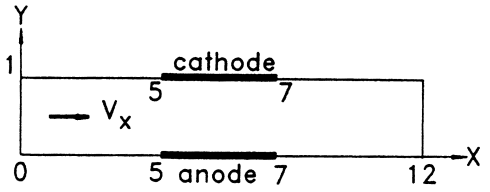

Fig. 9. Sketch of reactor for test 3.

An analytical solution to the problem can be derived following the same ideas as for the Leveque solution for parabolic flow [1] by assuming a semi-infinite electrode as a first approximation when the electrode length is very large compared to the cell width, and the convective velocity is also very large. For this, we take a convection-diffusion equation in a thin diffusion layer near the electrode, neglecting convection in the y-direction and considering the velocity constant in the x-direction, that is,

$$v\frac{\partial c}{\partial x} = D\frac{\partial^2 c}{\partial y^2} \tag{32}$$

This equation applies to a two-dimensional flow near the electrode with x measured along the electrode from its upstream end and y measured perpendicular from the surface into the solution.

The above partial differential equation has to satisfy the following boundary and asymptotic conditions:

$$c = 0 \quad \text{at} \quad y = 0 \quad \text{and} \quad \text{as} \quad x \to \infty$$
$$c = c_b \quad \text{at} \quad x = 0 \quad \text{and} \quad \text{as} \quad y \to \infty$$

To obtain the analytical solution, the following similarity variable is defined:

$$\epsilon = \frac{y}{2\sqrt{\beta x}}$$

in terms of the parameter $\beta = D/v$. In this way, the above boundary-value problem reduces to

$$c'' + 2\epsilon c' = 0$$

subject to $c = 0$ at $\epsilon = 0$ and $c = c_b$ as $\epsilon \to \infty$ (the prime denotes derivative with respect to the similarity variable ϵ).

Integrating twice the above ordinary differential equation and using the corresponding boundary conditions, we obtain

$$\frac{c}{c_b} = \frac{2}{\sqrt{\pi}}\int_0^{\epsilon} e^{-\eta^2} d\eta = \text{erf}(\epsilon)$$

By definition:

$$J_{\text{lim}} = -nFD\frac{\partial c}{\partial y}\bigg|_{y=0}$$

where

$$\frac{\partial c}{\partial y} = \frac{1}{2}\left(\frac{v}{Dx}\right)^{1/2} c'$$
$$c'\big|_{y=0} = A = \frac{2}{\sqrt{\pi}} c_b$$

So, finally we obtain

$$J_{\text{lim}} = -\frac{nFDc_{\text{b}}}{\sqrt{\pi}}\left(\frac{v}{Dx}\right)^{1/2}$$

Because the cathode only starts at position $x = 5$ (see Fig. 9), the analytical solution has to be shifted to this position, producing the final expression:

$$J_{\text{lim}} = -\frac{nFDc_{\text{b}}}{\sqrt{\pi}}\left(\frac{v}{D(x-5)}\right)^{1/2}$$

where J_{lim} is the limiting current density in A cm^{-2}.

Results are presented in Fig. 10 for several Péclet numbers. Because of the singularity of the current density at the leading edge of the electrodes ($x = 5$), the BEM solution produced some small oscillations at the first few points. These oscillations are not uncommon to BEM solutions, and were then treated with a standard algorithm previously used by Longuet–Higgins and Cokelet [19] to smooth the free surface of water waves. The smoothed current density distribution is shown in Fig. 11, where an excellent agreement with the exact solution can now be seen.

4.4. *Example 4*

In this test the BEM model is applied to a real size parallel plate cell with a ferri/ferrocyanide system and parabolic velocity distribution, and results compared to the Leveque solution. The geometry used for the numerical simulation is shown in Fig. 12. The length of the cathode and anode is 350 mm and the distance between the plates is 10 mm. At both inlet and outlet a 50 mm insulating part has been introduced to deal with the edge effects occurring at the electrodes.

The electrolyte is 0.005 M $K_4Fe(CN)_6^{3-}$, 0.01 M $K_4Fe(CN)_6^{4-}$ and 0.5 M NaOH at 20 °C. The physical properties of the electrolyte at this temperature are:

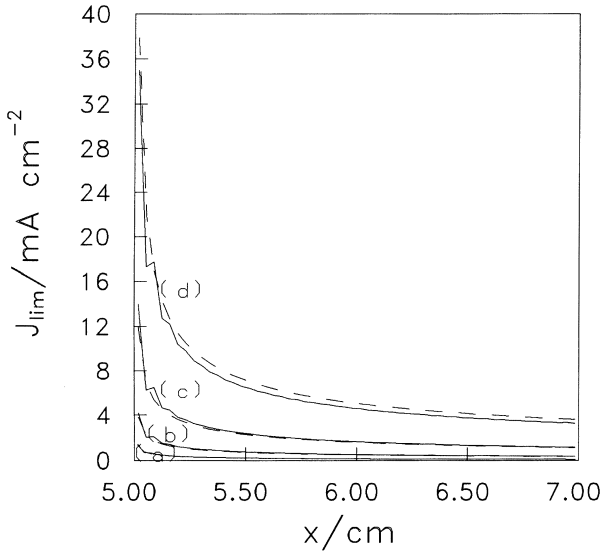

Fig. 10. Comparison between numerical and analytical results for current density distribution before smoothing, for different Péclet numbers. Analytical results (– – –); BEM results (——). *Pe*: (a) 417, (b) 4167, (c) 41 667 and (d) 416 667.

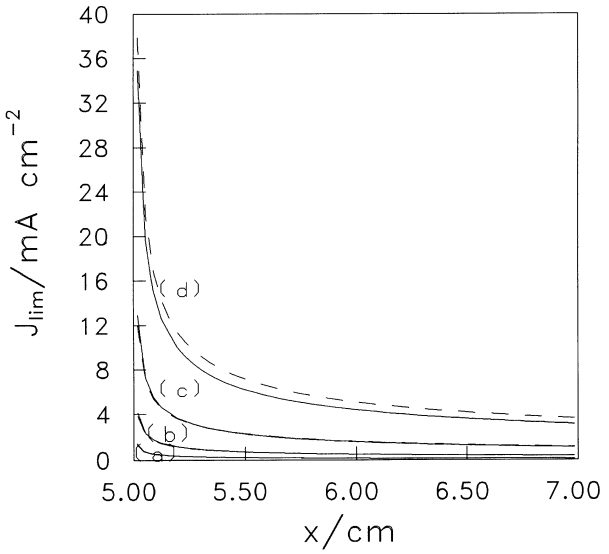

Fig. 11. Comparison between numerical and analytical results for current density distribution after smoothing, for different Péclet numbers. Analytical results (– – –); BEM results (——). *Pe*: (a) 417, (b) 4167, (c) 41 667 and (d) 416 667.

Density:

$$\rho = 1020.5\,\text{kg m}^{-3}$$

Viscosity:

$$\mu = 1.105 \times 10^{-3}\,\text{kg m}^{-1}\,\text{s}^{-1}$$

Diffusivity of ferricyanide ion:

$$D = 6.631 \times 10^{-10}\,\text{m}^2\,\text{s}^{-1}$$

resulting in a Schmidt number ($Sc = \mu/\rho D$) of 1633. The Reynolds number is defined as follows:

$$Re = \frac{d_{\text{e}}\langle v\rangle\rho}{\mu}$$

with $\langle v\rangle$ the average velocity and $d_{\text{e}} = 4wh/(w+h)$ the duct equivalent diameter depending on the height (h) and the width (w) of the cross section at the inlet of the channel. Since w in this case is 100 mm, this gives a value for d_{e} of 18.2 mm.

Comparison of results is shown in Figs 13 and 14 for Reynolds numbers of 55 and 180, corresponding to average velocities of $0.33\,\text{cm s}^{-1}$ and $1.08\ \text{cm s}^{-1}$ and Péclet numbers ($Pe = \langle v\rangle l/D$) of 2.2×10^6 and 7.3×10^6, respectively, taking the reference length l as the channel length 450 mm. Also shown in the Figures are the Leveque solutions [1]. The agreement between numerical and analytical solutions is reasonable for $Pe = 2.2 \times 10^6$; for $Pe = 7.3 \times 10^6$, the agreement is also reasonable apart from the vicinity

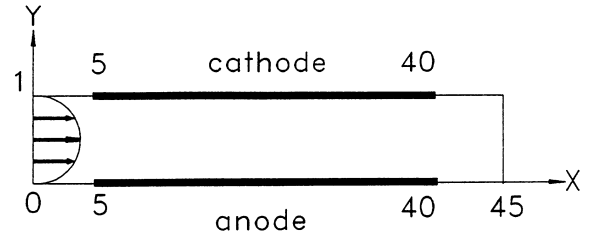

Fig. 12. Sketch of reactor for test 4.

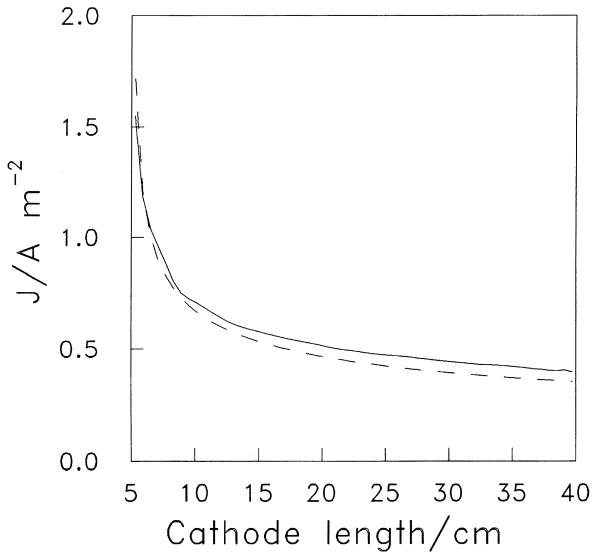

Fig. 13. Comparison between numerical and analytical results for current density ($Re = 55$). BEM results (——); analytical results (– – –).

of the leading edge of the electrode, where the BEM solution shows a steeper variation. Numerical solutions for higher Pe did not converge; therefore, the difference appears to be due to numerical errors in the BEM formulation. In this case, the discretization uses very thin cells near the electrode to capture the convective effects due to the flow boundary layers, generating integration problems for internal points located extremely close to the boundary.

5. Conclusions

This paper has described a numerical model, based on the boundary element method, for the calculation of concentration, potential and current density distributions in electrochemical cells controlled by diffusion, convection and migration. The formulation employs the complete Nernst–Planck equations and can deal with multiple ions and strongly nonlinear boundary conditions. The mathematical model employed reduces to a potential model in regions where the concentration of the ions is constant. Therefore, depending on the applied voltage, the current distributions obtained can vary from a secondary distribution up to a limiting current situation.

Some simple tests on parallel plate reactors have been investigated here, producing accurate results. We are now investigating the possibility of subdividing the flow region into subdomains to improve the accuracy of the formulation for very high Péclet numbers.

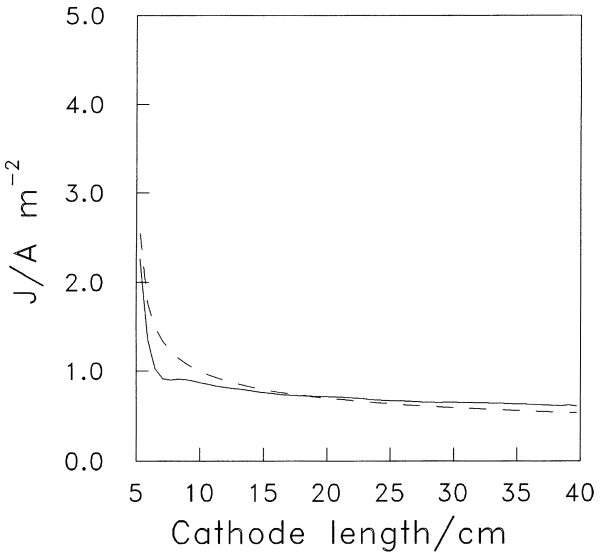

Fig. 14. Comparison between numerical and analytical results for current density ($Re = 180$). BEM results (——); analytical results (– – –).

Acknowledgements

This work forms part of the Brite–Euram project BE-5187, contract number BRE2–CT92-0170, funded by the European Commission. We thank our partners J. Deconinck and L. Bortels, from Vrije Universiteit Brussels, for supplying some of the numerical examples and their analytical and MDUM results. We also thank the referees for constructive comments on the original version of the paper.

References

[1] J. Newman, 'Electrochemical Systems', 2nd edn, Prentice-Hall, Englewood Cliffs, NJ (1991).
[2] R. Bialecki, R. Nahlik and M. Lapkowski, *Electrochim. Acta* **29** (1984) 905.
[3] J. Deconinck, G. Maggetto and J. Vereecken, *J. Electrochem. Soc.* **132** (1985) 2960.
[4] H. Kawamoto, *J. Appl. Electrochem.* **22** (1992) 1113.
[5] K. Bouzek, K. Borve, O. A. Lorentsen, K. Osmundsen, I. Rousar and J. Thonstad, *J. Electrochem. Soc.* **142** (1995) 64.
[6] L. Martens and K. Hertwig, *Electrochim. Acta* **40** (1995) 387.
[7] B. Steffen and I. Rousar, *ibid.* **40** (1995) 379.
[8] R. P. Buck, *J. Electroanal. Chem.* **271** (1981) 1.
[9] A. V. Sokirko, *ibid.* **364** (1994) 51.
[10] A. Katagiri, *J. Appl. Electrochem.* **21** (1991) 487.
[11] Y. I. Kharkats, A. V. Sokirko and F. H. Bark, *Electrochim. Acta* **40** (1995) 247.
[12] J. M. Bisang, *J. Appl. Electrochem.* **23** (1993) 966.
[13] L. Bortels and J. Deconinck, A new approach for solving mass and charge transport in electrochemical systems. Third European Symposium on Electrochemical Engineering, Nancy, France (1994).
[14] M. Georgiadou and R. Alkire, *J. Electrochem. Soc.* **141** (1994) 679.
[15] Z. H. Qiu, L. C. Wrobel and H. Power, *Enggn. Anal. Boundary elements* **15** (1995) 299.
[16] C. A. Brebbia, J. C. F. Telles and L. C. Wrobel, 'Boundary Element Techniques: Theory and Applications in Engineering', Springer-Verlag, Berlin (1984).
[17] J. Deconinck and L. Bortels, Final Project Report, Brite–Euram project BE-5187 (1995).
[18] J. P. S. Azevedo and L. C. Wrobel, *Int. J. Numer. Methods Eng.* **26** (1988) 19.
[19] M. S. Longuet-Higgins and E. D. Cokelet, *Proc. R. Soc. Lond.* **A350** (1976) 1.